UC San Diego
International Symposium on Stratified Flows

Title
Global patterns of internal wave variability from observations of full-depth rotary shear spectra

Permalink
https://escholarship.org/uc/item/0wj5z1sg

Journal
International Symposium on Stratified Flows, 8(1)

Authors
Waterhouse, Amy
Kunze, Eric
MacKinnon, Jennifer
et al.

Publication Date
2016-08-29

Global patterns of internal wave variability from observations of full-depth rotary shear spectra

Amy F Waterhouse[1], Eric Kunze[2], Jennifer A Mackinnon[1], Harper Simmons[3], Rob Pinkel[1], and Maxim Nikurashin[4]

[1]Scripps Institution of Oceanography, UCSD
San Diego, CA
awaterhouse@ucsd.edu

[2]Northwest Research Associates,
Redmond, WA

[3]University of Alaska Fairbanks,
Fairbanks, AK

[4]IMAS, University of Tasmania,
Hobart, Tasmania, Australia

Abstract

Internal waves are ubiquitous throughout the world ocean and are generated by a combination of processes including the tides and winds. The vertical directionality of low-frequency internal waves can be diagnosed by separating shear components into their rotary-with-depth components. Partitioning of energy in upward and downward propagation is helpful for understanding how energy is distributed and potentially lost in the global ocean energy budget. Using observations of horizontal velocity from the GO-SHIP surveys and interpreting North Hemisphere clockwise-with-depth (South Hemisphere counterclockwise-with-depth) signals as downward propagating, there is approximately 10% more downward than upward propagating shear variance at 120–320 m vertical wavelengths in the upper 2000 m. There is more upward and downward shear variance in the bottom 2000 m associated with rough topography.

1 Introduction

Internal waves in the ocean are generated by a variety of physical processes, including tidal flow over topography (Garrett and Kunze, 2007), winds generating near-inertial waves below the mixed layer (D'Asaro, 1985; Alford, 2001) and geostrophic flow over rough topography (Nikurashin and Ferrari, 2011; Melet et al., 2014). One of the largest outstanding questions remaining is where this energy goes after the internal waves propagate away from generation sites. The distance this energy travels directly determines the associated vertical structure of dissipation that ocean climate numerical models are sensitive (Melet et al., 2013, 2014, 2016). Through a limited number of observational studies, we have been able to make estimates on how far this energy propagation. However, there are relatively few of these process studies to make adequate global estimates. This work provides an opportunity to provide a larger constraint on how distribution of internal wave shear variance varies with depth and geographic location in the ocean.

Internal tides are generated by tidal flow over rough topography and can propagate in beams at knife-edge ridges (Althaus et al., 2003; St Laurent et al., 2003; Lee et al., 2006), which are directed upwards or downwards in the water column at angles defined by their characteristic slope (Munk, 1966; Baines, 1982; Egbert and Ray, 2000; Nycander,

2005). In regions of deep, rough topography, such as in the Brazil basin, nearly all of the shear variance propagates upwards as higher mode internal waves, slowly decaying as they propagate, which would appear as a preponderance of upward propagating shear variance at all depths.

Despite this, observations indicate downward propagating shear variance, which can be attributed to near-inertial waves (Alford and Gregg, 2001). Near-inertial waves propagate down from the mixed layer where they are generated by the wind in the form of long waves that travel long distances (Lueck and Reid, 1984; D'Asaro, 1985, 1995; Large and Crawford, 1995; Plueddemann and Farrar, 2006; Rimac et al., 2013) relatively quickly, in comparison to the slow-propagating higher-mode waves described above. The fate of these near-inertial waves is unknown but typically more downward (e.g. Kunze, 1985; Martini et al., 2014; Nagai et al., 2015) than upward (e.g. Waterman et al., 2013) propagating waves (with vertical wavelengths of near-inertial waves) have been observed from oceanic data sets.

Upward propagating waves can occur due tidal generation over rough topography (Shcherbina et al., 2003), from bottom bounces of tidal or near-inertial waves, or through other dynamics. The manner in which these waves propagate once their initial generation is a relative unknown. Determining the amount of energy that is partitioned between upward and downward propagating internal waves in the different ocean basins will help link the budget of wave generation, propagation to dissipation. Vertical wavenumber shear spectra are useful in constraining how energy is partitioned between upward and downward propagating internal waves (Shcherbina et al., 2003). In this work, we present rotary shear spectra from observations of full water column observations of shear to elucidate the global distribution of upward and downward propagating waves as well as the global distribution of these signals.

2   Observations

Rotary spectra of vertical profiles of shear were calculated from profiling LADCP profiles during the Global Ocean Ship-based Hydrographic Investigations Program (GO-SHIP) repeat hydrography cruises (Fig. 1). These data provide full-depth, global observations from the GO-SHIP surveys. Near-inertial internal waves have horizontal velocities describing a circle with time. If they are also vertically propagating, their velocities also describe a circle with depth. Rotary spectral decomposition was described by Gonella (1972) and Mooers (1973). Higher frequency internal waves are elliptical, and although the decomposition between upward and downward propagating components is not exact, the decomposition is still insightful. As both components of horizontal velocities are available from these GO-SHIP data, internal waves may be decomposed into motions with upwards and downwards group velocities following Leaman and Sanford (1975). In the northern hemisphere, counter-clockwise rotating waves are associated with upward group velocities while clockwise propagating waves are associated with downward group velocities. There are many caveats that must be considered with this analysis and these are discussed briefly in Section 3.3.

Full water column profiles of horizontal shear were obtained from 9714 Lowered ADCP (LADCP) profiles during the GO-SHIP hydrographic cruises from the Indian, Pacific, North Atlantic, and Southern Oceans between 1991 and 2011, covering nearly the full range of latitude and longitude (Kunze et al., 2006). Observations from GO-SHIP cruises have relatively more profiles taken from within the Indian Ocean (20°E to 60° E) as well
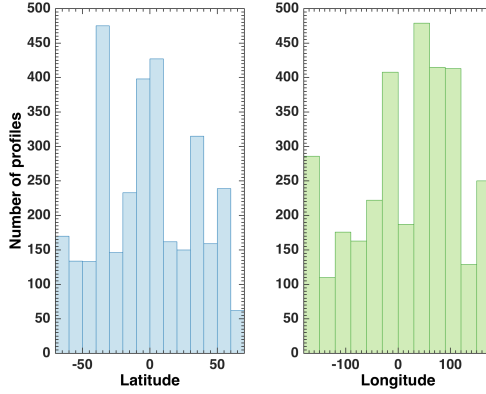
Figure 1: Total distribution of GO-SHIP CTD-LADCP profiles from in each bin of latitude and longitude for a total of 9714 profiles between 1991 and 2011.

as near the equator (10°S to 10°N; Fig. 1).

Velocity profiles from 300-kHz and 150-kHz lowered ADCPs, on 10- or 20-m-depth grids, were broken into half-overlapping 320-m-long segments. The segments were windowed at both ends with 10% $\sin^2$ tapers. Rotary shear spectra were formed from the Fourier coefficients normalized by the segment-averaged stratification, N [s^{-1}], and corrected for high-wavenumber attenuation with two sinc functions. Buoyancy-frequency normalized shear variances were then quantified by integrating the spectra from the minimum vertical wavenumber ($\lambda_z = 320$ m) to a maximum wavenumber ($\lambda_z = 150$ m) for both rotary components (clockwise and counter-clockwise). The narrow vertical wavenumber band (150 to 320 m wavelength) excludes both energy-containing and energy-flux containing low modes and the shear-variance-containing finescale. As such, this is intended to be an approximate measure of rotary-with-depth properties. Further details on the processing of the LADCP data can be found within Kunze et al. (2006).

The buoyancy-normalized-shear spectra of the clockwise-with-depth and counterclockwise-with-depth components are normalized by the Garrett-Munk shear spectra for an equivalent stratification. Following this, the mean of the buoyancy and GM normalized shear spectra are taken over three depth ranges: 1) from the surface down to 2000m, 2) the full water column and 3) from 1000 meters above bottom. These mean quantities are plotted over various latitudinal ranges to determine how shear variances change between clockwise- and counter-clockwise-with-depth components.

Following Leaman and Sanford (1975), the difference between the clockwise-with-depth and counterclockwise-with-depth shear spectra is interpreted as the net difference between downward- and upward-propagating internal waves under the assumptions that these signals are dominated by near-inertial frequencies. Although horizontal LADCP velocities may misrepresent the internal wave shear variance as a result of poor response at higher wavenumbers, the estimate of the clockwise and counterclockwise separation is consistent with that inferred from shipboard ADCP data (Shcherbina et al., 2003).

3   Results

3.1   Global patterns

In the upper 2000 m, there is on average 11% more downward than upward 150-320 m shear variance within 95% confidence intervals (upper panel of Fig. 2). This ratio varies
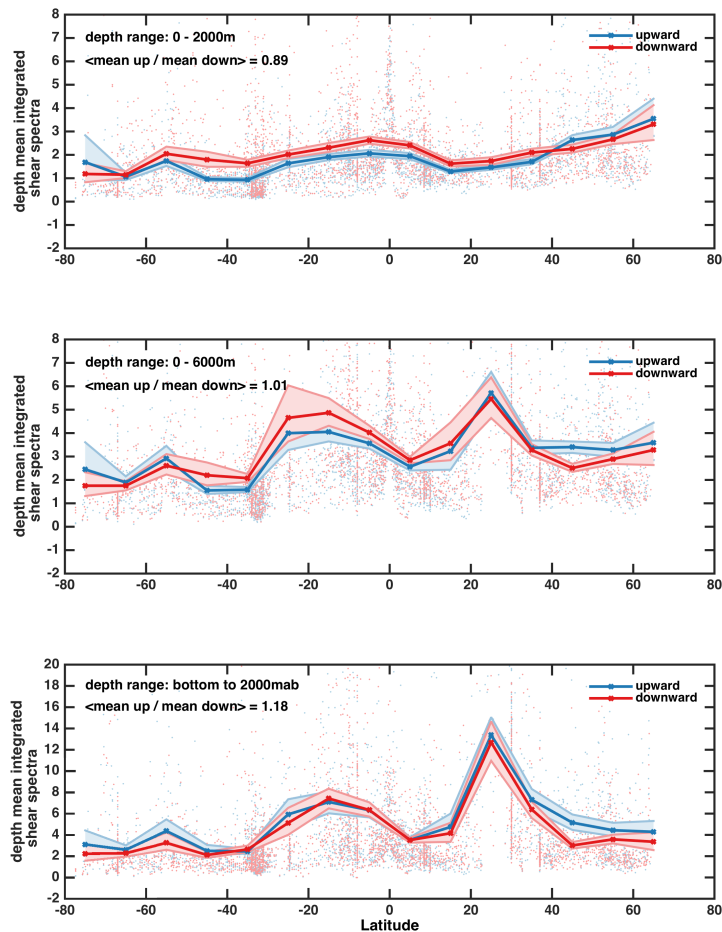
Figure 2: Binned integrated shear variance separated into depth ranges from (top) 0-2000m, (middle) full water column and (bottom) from 2000 meters above bottom (mab). Blue is upward propagating shear variance and red is downward propagating shear variance. Red and blue lines are averages over 10 degree bins and 95% bootstrap error bars are noted by the lighter shaded bands. Dots behind the solid lines indicate actual observations.

with latitude. In the full water column, (middle panel of Fig. 2), the ratio of clockwise-with-depth to counterclockwise-with-depth shear variance is not significantly different than one on average though upward exceeds downward at 45N. Shear variance peaks near 25°N and 25°S, equatorward of the peaks in wind power input at 40°N and 40°S as well as the 28 critical latitude for semidiurnal parametric subharmonic instability. In the bottom 2000 m of the water column (bottom panel of Fig. 2), there is 18% more upward than downward 150-320 m shear variance poleward of 35°N and 45°S.

3.2 Comparison to power input from tides, winds and lee waves

Rotary shear spectra are compared to the power input from tides, winds and lee waves from various locations along the GO-SHIP transects. While tide and wind power input far exceeds the power input from lee wave generation, only the comparison to lee wave generation is discussed here. The conversion of geostrophic flow into lee waves is estimated to account for 0.3 TW of internal wave power in the global ocean (Nikurashin and Ferrari, 2011). This estimate is based on a linear theory applied to bottom topography using single beam echosoundings, bottom stratification estimated from climatology, and bottom velocity obtained from a global ocean model. The total energy flux into internal lee waves is estimated to be 0.2 TW which is 20% of the global wind power input into the ocean.

Lee-wave generation is a regularly occurring event over isolated topographic regions (unlike wind events which are intermittent) and the power input from lee waves is compared to rotary-with-depth shear using individual GO-SHIP transects. Comparing two
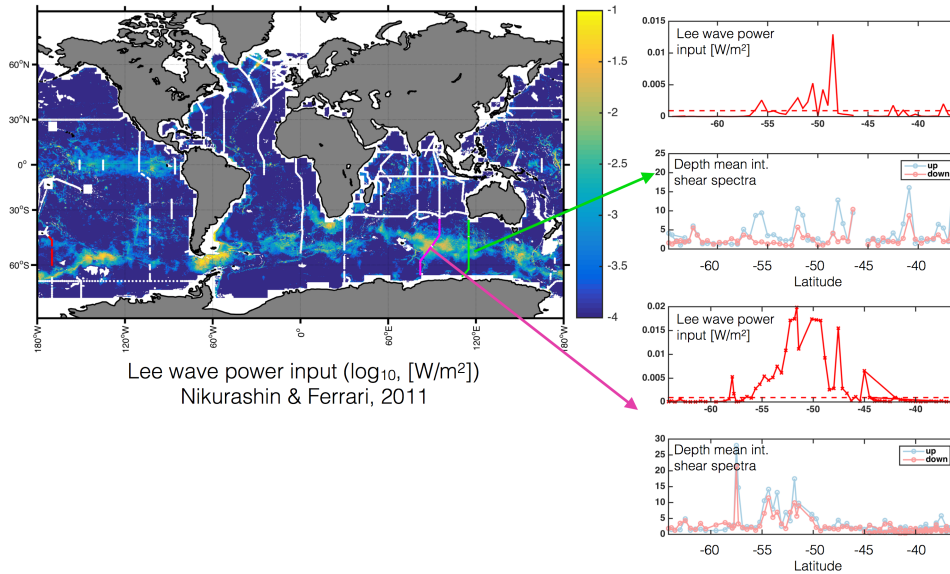
Figure 3: (left) Global map of the lee wave power input, from Nikurashin and Ferrari (2011) and (right) comparisons of the lee wave power input to two GO-SHIP sections. The two right hand panels show (top) the lee wave power input along the transect line with the global mean lee wave power input (red dashed line) and (bottom) the depth integrated upward (blue) and downward (red) components of the shear spectra from the bottom 1000m.

GO-SHIP transects in the Southern Hemisphere with lee-wave power input in two regions with high predicted generation (Fig. 3; Nikurashin and Ferrari, 2011), there is more clockwise-with-depth (upward) shear than counterclockwise in both locations.

3.3 Discussion

With further analysis of the data set provided by the GO-SHIP surveys, associations between wind and tidal input to rotary-with-depth shears will be detangled. The upper 2000 m exhibits peaks in shear variance near 20°N and 20°S with 11% more inferred downward than upward 150-320 m shear variance. In the bottom 2000 m of the water column, there is 18% more inferred upward than downward shear with no clear latitude dependence. Enhanced inferred clockwise-with-depth (upgoing) shear is found at two locations in the Southern Hemisphere where lee-wave generation is high.

There are a number of caveats that will be investigated further in performing this type of analysis. This include the fact that the internal tide, the largest internal wave source in the ocean, will generate upward rotary shear variances near rough topography that may also be associated with lee wave generation. Next, clockwise-with-depth and counter-clockwise-with-depth shear variances do not neglect standing waves which have equal portions of clockwise to counter-clockwise signals. Additionally, purely rotary-with-depth behavior is only found at the inertial frequency and wave motions become increasing rectified as frequency increases and net downward and upward energy cannot be directly equated to net downward and upward energy-flux (D'Asaro and Perkins, 1984). Finally, since the wavenumber band under consideration is very narrow (150 to 320 m wavelengths), this excludes both the energy-containing and energy-flux-containing low modes, and the finescale that dominates the shear.

References

Alford, M. H. (2001). Internal swell generation: The spatial distribution of energy flux from the wind to mixed layer near-inertial motions. *Journal of Physical Oceanography*, 31:2359–2368.

Alford, M. H. and Gregg, M. C. (2001). Near-inertial mixing: Modulation of shear, strain and microstructure at low latitude. *Journal of Geophysical Research*, 106(C8):16947–16916.

Althaus, A., Kunze, E., and Sanford, T. (2003). Internal tide radiation from Mendocino Escarpment. *Journal of Physical Oceanography*, 33(7):1510–1527.

Baines, P. G. (1982). On internal tide generation models. *Deep Sea Research Part A. Oceanographic Research Papers*, 29(3A):307–338.

D'Asaro, E. A. (1985). The Energy Flux From the Wind to Near-Inertial Motions in the Surface Mixed Layer. *Journal of Physical Oceanography*, 15(8):1043–1059.

D'Asaro, E. A. (1995). Upper-ocean inertial currents forced by a strong storm. III: Interaction of inertial currents and mesoscale eddies. *Journal of Physical Oceanography*, 25(11):2953–2958.

D'Asaro, E. A. and Perkins, H. (1984). A near-inertial internal wave spectrum for the Sargasso Sea in late summer. *Journal of Physical Oceanography*, 14(3):489–505.

Egbert, G. D. and Ray, R. D. (2000). Significant dissipation of tidal energy in the deep ocean inferred from satellite altimeter data. *Nature*, 405(6788):775–778.

Garrett, C. and Kunze, E. (2007). Internal Tide Generation in the Deep Ocean. *Annual Review of Fluid Mechanics*, 39(1):57–87.

Gonella, J. (1972). A rotary-component method for analysing meteorological and oceanographic vector time series. *Deep Sea Research*, 19:833–846.

Kunze, E. (1985). Near-Inertial Wave Propagation In Geostrophic Shear. *Journal of Physical Oceanography*, 15(5):544–565.

Kunze, E., Firing, E., Hummon, J. M., Chereskin, T. K., and Thurnherr, A. M. (2006). Global Abyssal Mixing Inferred from Lowered ADCP Shear and CTD Strain Profiles. *Journal of Physical Oceanography*, 36:1553.

Large, W. and Crawford, G. B. (1995). Observations and Simulations of Upper-Ocean Response to Wind Events during the Ocean Storms Experiment. *Journal of Physical Oceanography*, 25(11):2831–2852.

Leaman, K. D. and Sanford, T. B. (1975). Vertical energy propagation of interial waves: A vector spectral analysis of velocity profiles. *Journal of Geophysical Research*, 80(C):1975–1978.

Lee, C. M., Kunze, E., Sanford, T. B., Nash, J. D., Merrifield, M. A., and Holloway, P. E. (2006). Internal tides and turbulence along the 3000-m isobath of the Hawaiian Ridge. *Journal of Physical Oceanography*, 36(6):1165–1183.

Lueck, R. and Reid, R. (1984). On the production and dissipation of mechanical energy in the ocean. *Journal of Geophysical Research*, 89:3439–3445.

Martini, K. I., Simmons, H. L., Stoudt, C. A., and Hutchings, J. K. (2014). Near-Inertial Internal Waves and Sea Ice in the Beaufort Sea*. *Journal of Physical Oceanography*, 44(8):2212–2234.

Melet, A., Hallberg, R., Legg, S., and Nikurashin, M. (2014). Sensitivity of the Ocean State to Lee Wave–Driven Mixing. *Journal of Physical Oceanography*, 44(3):900–921.

Melet, A., Hallberg, R., Legg, S., and Polzin, K. L. (2013). Sensitivity of the Ocean State to the Vertical Distribution of Internal-Tide-Driven Mixing. *Journal of Physical Oceanography*, 43(3):602–615.

Melet, A., Legg, S., and Hallberg, R. (2016). Climatic impacts of parameterized local and remote tidal mixing. *Journal of Climate*, page in press.

Mooers, C. N. K. (1973). A technique for the cross spectrum analysis of pairs of complex-valued time series, with emphasis on properties of polarized components and rotational invariants. *Deep Sea Research and Oceanographic Abstracts*, 20:1129–1141.

Munk, W. H. (1966). Abyssal recipes. *Deep Sea Research*, 13(4):707–730.

Nagai, T., Tandon, A., Kunze, E., and Mahadevan, A. (2015). Spontaneous Generation of Near-Inertial Waves by the Kuroshio Front. *Journal of Physical Oceanography*, 45(9):2381–2406.

Nikurashin, M. and Ferrari, R. (2011). Global energy conversion rate from geostrophic flows into internal lee waves in the deep ocean. *Geophysical Research Letters*, 38:L08610.

Nycander, J. (2005). Generation of internal waves in the deep ocean by tides. *Journal of Geophysical Research*, 110(C10).

Plueddemann, A. J. and Farrar, J. T. (2006). Observations and models of the energy flux from the wind to mixed-layer inertial currents. *Deep Sea Research Part II: Topical Studies in Oceanography*, 53(1-2):5–30.

Rimac, A., Storch, J. S., Eden, C., and Haak, H. (2013). The influence of high–resolution wind stress field on the power input to near-inertial motions in the ocean. *Geophysical Research Letters*, 40(18):4882–4886.

Shcherbina, A. Y., Talley, L. D., Firing, E., and Hacker, P. (2003). Near-Surface Frontal Zone Trapping and Deep Upward Propagation of Internal Wave Energy in the Japan/East Sea. *Journal of Physical Oceanography*, 33:900–912.

St Laurent, L. C., Stringer, S., Garrett, C., and Perrault-Joncas, D. (2003). The generation of internal tides at abrupt topography. *Deep Sea Research Part I: Oceanographic Research Papers*, 50(8):987–1003.

Waterman, S., Naveira Garabato, A. C., and Polzin, K. L. (2013). Internal waves and turbulence in the Antarctic Circumpolar Current . *Journal of Physical Oceanography*, 43(2):259–282.